

### **3D joint inversion of magnetotelluric and magnetovariational data to image conductive anomalies in Southern Alberta, Canada**

*Michael R. Jorgensen, University of Utah, Martin Čuma and Michael S. Zhdanov, University of Utah and TechnoImaging*

#### **Summary**

It is well known that magnetotelluric (MT) impedance can be distorted by near-surface inhomogeneities (NSI), which complicates the interpretation of MT data and the correct imaging of deep geoelectrical structures. This paper demonstrates that the inclusion of magnetovariational (MV) tipper data in a three-dimensional (3D) inversion jointly with MT impedance provides better resolution of deep conductive anomalies than stand-alone MT impedance. This is significant because MV data can be collected alongside the MT impedance data for virtually no additional cost. Electric and magnetic fields in forward modeling are determined using the integral equation (IE) method. The inverse problem is solved with the re-weighted regularized conjugate gradient (RRCG) method with limited sensitivity domain. We present the results of both a synthetic model and case study using EarthScope data gathered in Southern Alberta, Canada. In both cases, the joint inversion provides more accurate information about deep conductive anomalies than the inversion of impedance stand-alone data.

#### **Introduction**

The MT method as developed by Tikhonov and Cagniard in 1950 and 1953, respectively, produces a geoelectrical model of the earth via inversion of MT impedance, which is simply a ratio of the earth's ambient electric and magnetic fields measured over some range of periods. Rapid advances in parallel computing and data acquisition over the last few decades have elevated the MT method to practicality. 2D interpretations—which were often patchworks of 1D interpretations stitched together from sparse data and insufficient to describe complex geoelectrical models—have made way to full-fledged 3D interpretations; however, 3D MT inversion still suffers from the problem of NSI (Chave and Jones, 2012). A horizontal inhomogeneity near the receivers leads to a build-up of charge and a localized distortion in the electric field, which corrupts data about deeper geoelectrical structure via galvanic static shifts (Berdichevsky and Dmitriev, 1976). The magnetovariational (MV) method as developed by Parkinson (1950) and Wiese (1962), respectively, utilizes a vertical transfer function with respect to the magnetic field known as the tipper. Joint 3D inversion of MT impedance and MV tipper data can correct for these static shifts, as the tipper is far less susceptible to distortion due to NSI (Berdichevsky and Dmitriev, 2002).

Finite-difference (FD), finite-element (FE), and finite-volume (FV) methods in forward modeling have been favored for models anticipated to be geologically complex, and conversely, IE methods have been favored for a small number of anticipated anomalous bodies. This is due to the IE method discretizing only over the anomalous domain. Advances by Zhdanov et al. (2006) have made IE more practical for complex structures, while maintaining computational efficiency. A review of FD, FE, and FV methods can be found in Chave and Jones (2012).

A good review of generalized formalism for electromagnetic inversion is found in Egbert and Kelbert (2012). It highlights the recent trend of inversion algorithms using an alternative to solving for a quadratic approximation of a parametric functional using an iterative Gauss-Newton scheme: directly minimizing the parametric functional using a more memory-efficient Krylov-space solver such as conjugate gradients. This study uses the RRCG method with adaptive regularization and both quasi-Born approximation and limited sensitivity domain to assist in computation of the Fréchet (sensitivity) matrices (Zhdanov, 2002; 2009). Data weights are based on variance and the misfit is reported as root mean squared (RMS).

#### **Modeling methodology**

We employ the frequency-domain contraction integral equation (IE) method (Hursan and Zhdanov, 2002; Zhdanov, 2002, 2009). The total fields are decomposed into primary (background) and secondary (anomalous) fields. These decomposed fields are substituted into harmonic time-dependent forms of Ampere's and Faraday's laws, and by applying electromagnetic Green's functions, one can find the observations fields at the receiver locations generated by the surface currents in some inhomogeneous domain (Hohmann, 1975; Warnick and Arnold, 1996).

#### **Inversion methodology**

As discussed above, the presence of NSI can significantly distort the measured electric field at the surface and cause static shifts of apparent resistivity curves over all frequencies. This phenomenon is one of the major problems in interpretation of MT data. Berdichevsky and Dmitriev (2002) suggested a joint inversion of MT and MV data, suggesting that MV data are not nearly as susceptible to distortions due to NSI. The following combined

### 3D joint inversion applied to Southern Alberta, Canada

parametric functional was introduced (Zhdanov et al., 2010) to jointly minimize the misfit between observed and predicted data:

$$P(\mathbf{m}, \mathbf{d}) = \phi^{MT}(\mathbf{m}, \mathbf{d}) + \phi^{MV}(\mathbf{m}, \mathbf{d}) + \alpha s(\mathbf{m}) = \min$$

$$\phi^{MT(MV)}(\mathbf{m}, \mathbf{d}) = \left\| \mathbf{W}_d^{MT(MV)} (\mathbf{A}^{MT(MV)}(\mathbf{m}) - \mathbf{d}^{MT(MV)}) \right\|^2$$

$$s(\mathbf{m}) = \left\| \mathbf{W}_m (\mathbf{m} - \mathbf{m}_{apr.}) \right\|^2,$$

where  $\mathbf{A}$  is the forward modeling operator,  $\mathbf{m}$  is the model parameters,  $\mathbf{d}$  is the data,  $\phi$  are the weighted misfit functionals describing the norm square of the difference between the observed and predicted data,  $s$  is the minimum norm stabilizing functional,  $\alpha$  is the regularization parameter, and  $\mathbf{W}$  are the weighting matrices. The *apr* subscript indicates model information that is known a priori. The parametric functional is minimized using the RRCG method outlined in Zhdanov (2009).

Weighting matrices are important elements in geophysical inversion. Unweighted geophysical inversions often yield information about shallow anomalies only, while the inclusion of weights can reveal deeper geological features as well (Zhdanov, 2002). The model weighting matrix is a diagonal matrix determined by:

$$\mathbf{W}_m = \text{diag} \left( \sqrt[4]{\mathbf{F}^* \mathbf{F}} \right),$$

where  $\mathbf{F}$  is the Fréchet derivative of  $\mathbf{A}$  with respect to  $\mathbf{m}$ , and  $\mathbf{F}^*$  is the transposed complex conjugate of  $\mathbf{F}$ . The data weighting matrices are populated using supplied variance information. The scalar components of the data weighting matrices are scaled by the square root of the variance, unless the variance falls beneath a predefined error floor.

The Fréchet derivative matrix can become prohibitively large for large-scale 3D inversions, often consisting of millions of cells. The calculation of inducing currents in cells far away from the receivers is often unnecessary, as those currents will have a negligible effect on the fields near the receivers. As such, Cox and Zhdanov (2007) developed a limited sensitivity domain (LSD) approach to the calculation of the Fréchet derivative matrix. This approach was later adapted to MT inversion by Zhdanov et al. (2010) and Gribenko et al. (2010). Only cells within a predefined distance, based upon the skin depth, are included in calculation of the Fréchet derivative. All others are set to zero. In this study, the LSD is predefined to include all cells within three times the skin depth. It is important to note that the LSD is only used in the calculation of the Fréchet derivatives. The calculations of

the predicted data for the MT impedance and MV tipper are rigorous to ensure the accuracy of the result.

#### Synthetic Model Study

This model study demonstrates the feasibility of the developed joint inversion methodology. The model consists of a homogeneous 1000 Ohm-m half-space, a 10 Ohm-m anomalous L-shaped body, and significant NSI. 5% noise was also added to the fields. The MT and MV data in this feasibility study are computer simulated at 81 stations, which are spaced equidistantly at 1000 m intervals in the X and Y directions on a flat surface with no topography. Eight frequencies are used in the range from 0.01 Hz to 20 Hz. This frequency range corresponds to a depth of investigation down to approximately 50 km in a 1000 Ohm-m host medium. The inversion domain in the X, Y, and Z directions extends to 10.5 km, 10 km, and 4.1 km, respectively. The horizontal cell size is 250 m by 250 m with a uniform vertical discretization of 100 m. The inversion domain contained 67,200 cells. The misfit cutoff was set at the noise level.

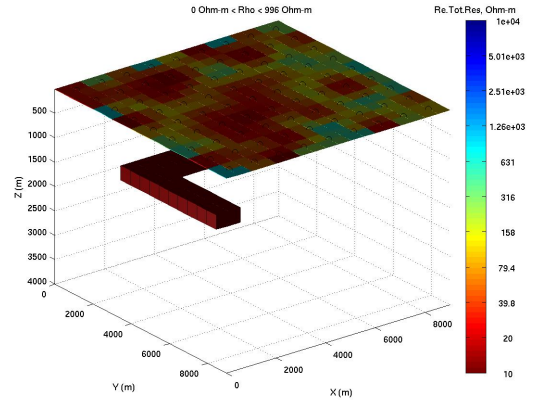


Figure 1: True model from the Synthetic Model Study. The background resistivity (1000 Ohm-m) has been omitted for clarity.

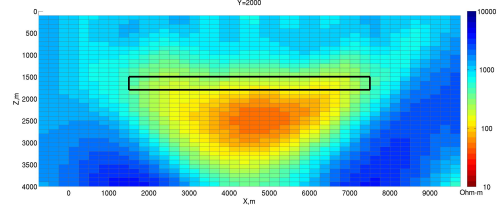


Figure 2: Vertical resistivity section of the Synthetic Model Study using only full impedance field components. The true location of the 10 Ohm-m anomalous body is outlined in black.

### 3D joint inversion applied to Southern Alberta, Canada

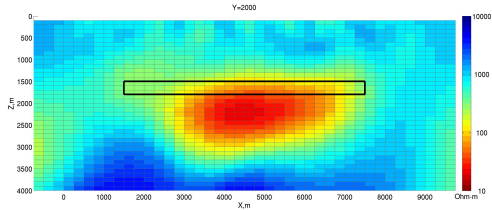


Figure 3: Vertical resistivity section of the Synthetic Model Study using full impedance and tipper field components. The true location of the 10 Ohm-m anomalous body is outlined in black.

The addition of tipper field components to impedance field components produced more accurate inversion results than inversions of impedance data alone. A clear drawback to the MT method is apparent in the models: information directly underneath strong conductors is often distorted due to the diffusive dissipation of energy in the conductor.

#### Case Study: Southern Alberta, Canada

The MT data set analyzed here was gathered in southern Alberta, Canada. Data was acquired by the EarthScope program using long-period fluxgate magnetometers.

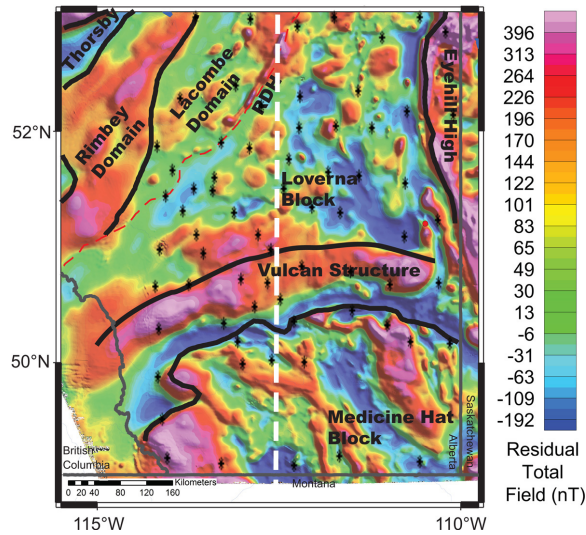


Figure 4: Aeromagnetic map of the survey area with interpreted tectonostratigraphic boundaries (modified from Nieuwenhuis et al., 2014; Geological Survey of Canada, 2011). Black asterisks indicate station locations. The white dashed line indicates the location of the vertical resistivity sections. RDH is the Red Deer High.

The Western Canadian Sedimentary Basin (Proterozoic or Phanerozoic) overlays Archean and Proterozoic basement blocks, which are thought to have been sutured together

during the Proterozoic eon (Hoffman, 1989). Understanding of this basement structure is limited due to the 2-3 km thick overlying sedimentary basin (Nieuwenhuis et al., 2014). A priori knowledge is based primarily on various geophysical studies carried out in the region (Boerner et al., 1995, 2000; Gorman et al., 2002; Nieuwenhuis et al., 2014). These studies have identified several conductive anomalies in the otherwise resistive crystalline basement blocks. Two of these conductive anomalies—an anomaly in the upper mantle beneath the Archean Loverna Block and a crustal anomaly coincident with the Red Deer High—are the targets in this study.

The Loverna Conductor was likely formed during the Proterozoic assembly of Laurentia. A northward or southward dipping subduction zone is believed to have formed the Vulcan Structure (Hoffman, 1988): a tectonic suture between the Loverna and Medicine Hat Blocks. This tectonic activity possibly enriched the upper mantle coincident with the Loverna Conductor with carbon, which would later have formed graphite films on grain boundaries (Nieuwenhuis et al., 2014; Selway, 2014).

The Red Deer Conductor is coincident with a thin magnetic high relating to high iron content on the eastern edge of the Lacombe Domain. This feature has been interpreted as a foredeep structure also related to Proterozoic subduction within Alberta, and is thought to be comprised of multiple discrete conductors (Boerner et al., 1995) also graphitic in nature. There is significant uncertainty as to whether the Loverna and Red Deer Conductors merge at some point.

#### Inversion parameters

87 MT stations were used in the inversion. Station spacing is roughly 25 km. A total of 24 interpolated frequencies are used over the period range 1-10,000 s. This frequency range corresponds to a depth of investigation down to 500 km in a 100 Ohm-m host medium. This half-space was selected based upon 1D MT inversion. The inversion domain in X, Y, and Z spans 400 km, 600 km, and 500 km, respectively. The X and Y cell sizes are discretized at 10 km by 10 km, with a vertical discretization ranging from 0.5-32 km comprised of 64 Z-layers logarithmically increasing with depth. The inversion domain contained 101,824 cells. The limited sensitivity domain was set to 3 times skin depth. Error floors were 10% for MT impedance components and 0.06 for MV tipper components. These relatively large error floors were selected to compensate for a large XY/YX split in the impedance data. The inversions were allowed to iterate until the RMS misfit converged and failed to decrease by 0.01 over a span of 10 iterations. A total of 12 sixteen-core nodes were used, splitting the work into 48 MPI processes, each of which ran 4 Open MP threads. The typical runtime was approximately 6 hours.

## 3D joint inversion applied to Southern Alberta, Canada

### Results

The iterative stopping criterion was met at 85 iterations for the full impedance only inversion. It converged to an RMS misfit of 2.16. In contrast, the full impedance plus tipper inversion converged after 159 iterations to a misfit of 2.41.

It is clear in the vertical resistivity sections below that the inclusion of the tipper data significantly limited diffusive MT distortion of deep conductors. In the joint result, the conductive anomaly underlying the Loverna Block is coincident with the Deep Probe seismic reflector f1 (Gorman et al., 2002). The joint result is also best constrained by the carbon phase transition indicated in the vertical sections (Nieuwenhuis et al., 2014), and is consistent with an interpretation of graphitic enrichment associated with subduction (Selway, 2014).

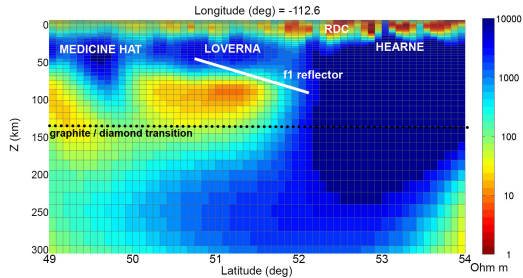


Figure 5: Vertical resistivity section of the Case Study using only full impedance field components. The solid white line is the seismic reflector f1 from the Deep Probe Velocity Model reported in Gorman et al. (2002). The black dotted line is the approximate depth of the diamond/graphite phase transition for the region. RDC is the Red Deer Conductor.

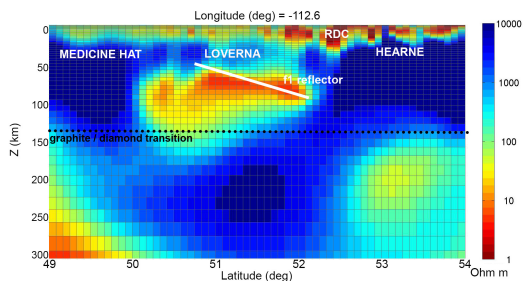


Figure 6: Vertical resistivity section of the Case Study using full impedance and tipper field components. The solid white line is the seismic reflector f1 from the Deep Probe Velocity Model reported in Gorman et al. (2002). The black dotted line is the approximate depth of the diamond/graphite phase transition for the region. RDC is the Red Deer Conductor.

Anomalous crustal conductors coincident with the Red Deer High are recovered in both results; however, the question of whether the Loverna and Red Deer Conductors merge is ambiguous. The joint result tends to indicate a possible merger around the Moho, but it is possible this is a diffusive effect of the inversion.

### Conclusions

We have outlined methods of forward modeling and joint inversion of magnetotelluric and magnetovariational data. We have illustrated these methods in a Model Study using synthetic data and a Case Study using EarthScope data gathered in Southern Alberta, Canada. We presented inversions of impedance alone versus inversions of impedance and tipper data. In both cases, the joint inversions provided additional information about the shape and locations of deep conductive anomalies. In the Case Study, one can see that both the impedance and joint impedance plus tipper inversions resolve the target anomalies to some degree. The Red Deer Conductor appears as a set of discrete conductors in the upper crust and the Loverna Conductor appears as a continuous conductor in the upper mantle; however, the Loverna Conductor is only well constrained by seismic, geochemical, and interpreted tectonostratigraphic boundaries in the joint inversion. Moreover, the depth resolution of the Red Deer Conductor is clearest in the joint result, and sharp contrast is best resolved through the diffusive MT effect attributed to the overlying sedimentary basin. Both anomalies are consistent with graphite films on grain boundaries. Although a tenuous connection of the anomalies is visible in the joint result, it is our interpretation that this is simply the diffusive MT effect, and that the anomalies do not necessarily merge in a geophysically meaningful way.

Both Boerner et al. (2000) and Nieuwenhuis et al. (2014) reported phenomena in 2D inversions where crustal conductors moved after inclusion of the tipper data, and interpreted this as evidence of either crustal anisotropy or unstable model features. These shifting phenomena did not appear in our joint inversion result, and this would tend to indicate that the crustal conductors are stable model features.

### Acknowledgements

The authors acknowledge the support of the University of Utah Consortium for Electromagnetic Modeling and Inversion (CEMI) and TechnoImaging. We also acknowledge the Extreme Science and Engineering Discovery Environment (XSEDE) for providing computational resources and Alexander Gribenko for his assistance with this project.

## References

- Berdichevsky, M. N., V. I. Dmitriev, 1976, Distortion of magnetic and electrical fields by near-surface lateral inhomogeneities: *Acta Geodaetica*, **11**, 447-483.
- Berdichevsky, M. N., and V. I. Dmitriev, 2002, Magnetotellurics in the context of the theory of ill-posed problems: Society of Exploration Geophysicists.
- Boerner, D. E., R. D. Kurtz, J. A. Craven, S. Rondenay, and W. Qian, 1995, Buried Proterozoic foredeep under the Western Canadian Sedimentary Basin? *Geology*, **23** (4), 297-300.
- Boerner, D. E., R. D. Kurtz, J. A. Craven, G. M. Ross, and F. W. Jones, 2000, A synthesis of electromagnetic studies in the Lithoprobe Alberta Basement Transect: constraints on Paleoproterozoic indentation tectonics: *Canadian Journal of Earth Sciences*, **37** (11), 1509-1534.
- Cagniard, L., 1953, Basic theory of the magnetotelluric method of geophysical prospecting: *Geophysics*, **18**, 605-635.
- Chave, A. D., and A. G. Jones, 2012, *Introduction to the magnetotelluric method*: Cambridge University Press.
- Cox, L. H., and M. S. Zhdanov, 2007, Large scale 3D inversion of HEM data using a moving footprint: 77th Annual International Meeting, SEG, Expanded Abstracts, 467-471.
- Egbert, G. D., and A. Kelbert, 2012, Computational recipes for electromagnetic inverse problems: *Geophysical Journal International*, **189**, 251-267.
- Geological Survey of Canada, 2011, Canadian Aeromagnetic Data Base, Airborne Geophysics Section, GSC: Central Canada Division, Geological Survey of Canada, Earth Sciences Sector, Natural Resources Canada.
- Gorman, A.R., R.M. Clowes, R.M. Ellis, T.J. Henstock, G.D. Spence, G.R. Keller, A. Levander, C.M. Snelson, M.J.A. Buriannyk, E.R. Kanasevich, I. Asudeh, Z. Hajnal, and K.C. Miller, 2002, Deep probe: imaging the roots of western North America: *Canadian Journal of Earth Sciences*, **39** (3), 375-398.
- Gribenko, A., and M.S. Zhdanov, 2007, Rigorous 3D inversion of marine CSEM data based on the integral equation method: *Geophysics* **72**, WA73-WA74.
- Gribenko, A., A. M. Green, M. Čuma, and M. S. Zhdanov, 2010, Efficient 3D inversion of MT data using integral equation method and the receiver footprint approach: application to the large-scale inversion of the Earthscope MT data: 80th Annual International Meeting, SEG, Expanded Abstracts, 644-649.
- Hoffman, P. F., 1988, United States of America, the birth of a craton: early Proterozoic assembly and growth of Laurentia: *Annual Review of Earth and Planetary Sciences*, **16** (1), 543-603.
- Hoffman, P. F., 1989, Speculations on Laurentia's first gigayear (2.0 to 1.0 Ga): *Geology*, **17** (2), 135-138.
- Hohmann, G. W., 1975, Three-dimensional induced polarization and EM modeling: *Geophysics*, **40**, 309-324.
- Hursan, G., and M. S. Zhdanov, 2002, Contraction integral equation method in three-dimensional electromagnetic modeling: *Radio Science*, **37** (6), 1089.
- Nieuwenhuis, G., M. J. Unsworth, D. Pana, J. Craven, and E. Bertrand, 2014, Three-dimensional resistivity structures of Southern Alberta, Canada: implications for Precambrian tectonics: *Geophysical Journal International*, **197** (2), 731-747.
- Parkinson, W. D., 1959, Direction of rapid geomagnetic fluctuation: *Geophysical Journal of the Royal Astronomical Society*, **2** (1), 1-14.
- Selway, K., 2014, On the causes of electrical conductivity anomalies in tectonically stable lithosphere: *Surveys in Geophysics*, **35**, 219-257.
- Tikhonov, A. N., 1950, On determining electrical characteristics of the deep layers of the Earth's crust: *Doklady*, **73**, 295-297.

- Warnick, K. F., and D. V. Arnold, 1996, Electromagnetic Green functions using differential forms: *Journal of Electromagnetic Waves and Applications*, **10** (3), 427-438.
- Wiese, V. H., 1962, Geomagnetic tiefentellurik part II: the strike of the underground structures of the electrical resistance, inferred from geomagnetic variations: *Pure and Applied Geophysics*, **52** (1), 83-103.
- Zhdanov, M. S., 2002, *Geophysical inverse theory and regularization problems*: Elsevier.
- Zhdanov, M. S., 2009, *Geophysical electromagnetic theory and methods*: Elsevier.
- Zhdanov, M. S., S. K. Lee, and K. Yoshioka, 2006, Integral equation method for 3D modeling of electromagnetic fields in complex structures with inhomogeneous background conductivity: *Geophysics*, **71**, G333-G345.
- Zhdanov, M. S., V. I. Dmitriev, and A. V. Gribenko, 2010, Joint three-dimensional inversion of magnetotelluric and magnetovariational data: *Physics of the Solid Earth*, **46** (8), 655-669.